

CLASSIFICATION OF GROUND DEFORMATION IN InSAR DATA USING CNNs.

Under the supervision of
Prof. PABITRA MITRA, - April 2019
Dept. of Computer Science and Engineering
IIT-Kharagpur

and

Mr.Kaushik Biswas(Ph.D),
Under
Prof.Pabitra Mitra, Dept. CSE
Prof.Debashish Chakravarty
Dept. Mining Engineering

Report by:
P. JAYANTH AVINASH,15EE10029
4th year UG student, Dept. of Electrical Engineering



1 DECLARATION and ACKNOWLEDGEMENT

I certify that

- (a) The work contained in this report has been done by me under the guidance of my supervisor.
- (b) The work has not been submitted to any other Institute for any degree or diploma.
- (c) I have conformed to the norms and guidelines given in the Ethical Code of Conduct of the Institute.
- (d) Whenever I have used materials (data, theoretical analysis, figures, and text) from other sources, I have given due credit to them by citing them in the text of the thesis and giving their details in the references. Further, I have taken permission from the copyright owners of the sources, whenever necessary.

I would like to express gratitude and indebtedness to my supervisor Prof. Pabitra Mitra, Computer Science and Engineering Department, IIT Kharagpur, Mr. Koushik Biswas, and Prof. Debashish Chakravarthy for their guidance and encouragement in the present investigation throughout the duration of this project. It is beyond doubt that this work would not have come into existence in the absence of their guidance.

I express my sincere thanks to all my professors for their encouragement at different stages of my work.

P.JAYANTH AVINASH,15EE10029

CERTIFICATION



This is to certify that the project report entitled “CLASSIFICATION OF GROUND DEFORMATION IN InSAR DATA USING CNNs.” submitted by P. JAYANTH AVINASH (Roll No. 15EE10029) to Indian Institute of Technology Kharagpur towards partial fulfillment of requirements for the award of degree of Bachelor of Technology in Electrical Engineering is a record of bonafide work carried out by him under my supervision and guidance during spring Semester, 2018-19.

Prof. Pabitra Mitra,
Dept. of Computer Science and Engineering
IIT Kharagpur

Contents

1	DECLARATION and ACKNOWLEDGEMENT	1
2	INTRODUCTION	4
3	INTERFEROMETRY	5
4	DATA and EXPERIMENTATION	5
4.1	Our data and Preparation	7
4.2	Challenges involved	8
5	LITERATURE REVIEW	8
5.1	Hyper-parameters	8
5.2	Activations	9
5.3	DropOut	9
5.4	Transfer learning	10
5.5	SPPNet	10
5.6	CNN Models used and their Architectures	11
5.6.1	AlexNet	14
5.6.2	VGG16	14
5.6.3	InceptionV3	15
5.6.4	ResNet50	18
5.6.5	DenseNet121	20
6	HARWARE ACCELERATORS and LIBRARIES	21
7	RESULTS	22
8	Inference and Continuation of work..	27
9	References	28

2 INTRODUCTION

Recent improvements in the frequency, type, and availability of satellite images made it feasible to routinely study volcanoes in remote and inaccessible regions, including those with no ground-based monitoring. In particular, Interferometric Synthetic Aperture Radar data can detect surface deformation, which has a strong statistical link to eruption[10]. However, the data set produced by the recently launched Sentinel-1 satellite is too large to be manually analyzed on a global basis. In this study, we systematically process $\geq 30,000$ short-term interferograms at over 900 volcanoes and apply machine learning algorithms to automatically detect volcanic ground deformation. Here, use Different well-known CNN Architectures and use them to classify the interferograms. We use a transfer learning strategy and study the performance of Networks for some specific learning rates and optimizers.

Globally, 800 million people live within 100 km of a volcano. Improvements in monitoring and forecasting have been shown to reduce fatalities due to volcanic eruptions, but a significant proportion of the $\sim 1,500$ Holocene volcanoes have no ground-based monitoring[10]. Interferometric Synthetic Aperture Radar (InSAR) is a satellite remote sensing technique used to measure ground displacement at the centimeter scale over large geographic areas and has been widely applied to volcanology (e.g., Biggs Pritchard, 2017; Pinel et al., 2014). Furthermore, InSAR measurements of volcanic deformation have a significant statistical link to eruption. Modern satellites provide large coverage with high-resolution signals, generating large data sets. For example, the two-satellite constellation, Sentinel-1 A and B, offers a 6-day repeat cycle and acquires data with a 250-km swath at a 5 m by 20 m spatial resolution (single look)[10]. This amounts to ≥ 10 -TB per day or about 2 PB collected between its launch in 2014 and June 2017. The explosion in data has brought major challenges associated with the manual inspection of imagery and timely dissemination of information. Many volcano observatories lack the expertise needed to exploit satellite data sets, particularly those in developing countries.

Similarly, Deformation occurring due to mining activity will have a considerable effect on fatalities. In this project, we develop study CNN models and study their effectiveness in Classifying small scale Deformation(due to mining activity). The Major Challenge in our case is that Deformation fringes in Interferograms are much less pronounced than in the case of Volcanic deformation. Also, the shape and size of Deformation fringes in Small Scale Deformation (SSD) vary largely across the different interferograms since they are consequences of human activity, unlike Volcanoes. Most importantly the size of Data available for SSD (for training CNNs) is comparatively much lesser than the case of Volcanic data, so currently the data preparation for our case is in process and Networks are Trained on Volcanic data in order to study their performances beforehand(since SSD is similar to Large Scale Deformation; LSD to some Extent).

3 INTERFEROMETRY

Interferometry is a Class of scientific techniques used to Extract information by the phenomenon of interference caused when Electromagnetic waves superimpose on each other. These techniques use two or more Synthetic Aperture Radar (SAR) images to generate maps of surface deformation or digital elevation using differences in phase of the waves returning to the satellite[11]. Interferograms help us to determine the location, magnitude, and type of an earthquake. They can also help us to improve earthquake models, and investigate the future seismic hazard for an area. The most important factor affecting the phase is the interaction with the Ground surface. The phase of the wave may change on reflection depending on the properties of the material.

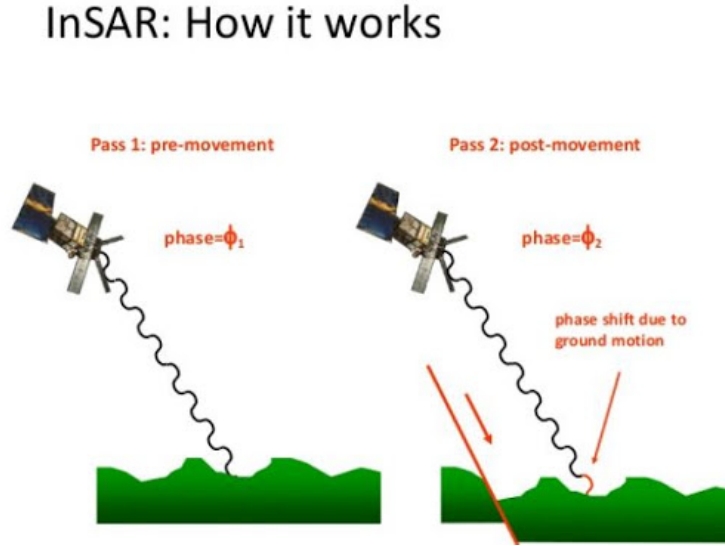


Figure 1: Picture showing Master-slave configuration where Two pictures of the same area taken with time certain cycle by two satellites @ source: science direct

There are basically two images obtained which differ by some phase difference(due to deformation, atmospheric noise, etc) and are mapped from $[\phi_1 - \phi_2]$ to 0-256(RGB) for displaying. In case Wrapped phase interferograms $[\phi_1 - \phi_2]$ is wrapped to $[0 - 2\pi]$, which is again mapped to 0-256(RGB).

4 DATA and EXPERIMENTATION

In this project we worked with wrapped phase interferograms. The values of wrapped interferograms vary between $-\pi$ and π and they are typically displayed with colors (red, green, and blue intensities).

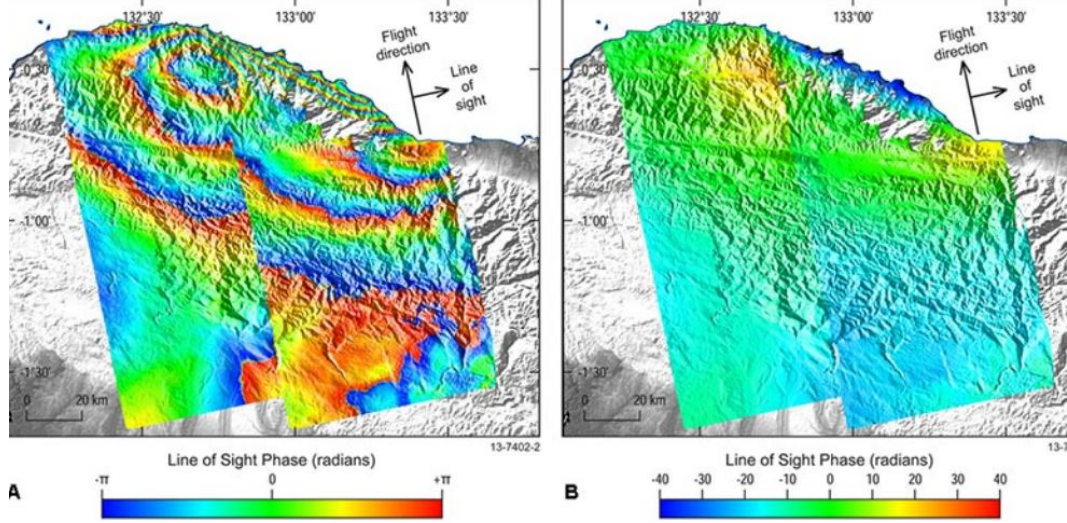


Figure 2: (A)wrapped and (B)unwrapped-phase Interferograms, source: Geoscience Australia

For the sake of using Convolutional Neural Nets(CNNs), we first convert the wrapped interferogram into a grayscale image, that is, the pixel value in the range of $[-\pi, \pi]$ is scaled to $[0, 255]$ or $[125, 125]$ if zero-center normalization is required. Subsequently, each training image is divided into patches equal to the input size of the CNNs (mostly 224×224). In the case of Volcanic deformation Data(LSD), Canny edge detection is applied, where a Gaussian filter is first applied to remove noise, and then double thresholding is applied to the intensity gradients of the image. As the wrapped-phase interferograms show strong edges where the phase jumps between $-\pi$ and π the Canny operator can straightforwardly extract fringes occurring from volcano deformation[10]. As the number of background areas (negative samples) is significantly larger than those associated with volcano deformation (positive samples), only the patches in which strong edges have been detected are used. Since areas without strong edges are unlikely to contain volcanic deformation, they are instantly defined as backgrounds without classification by CNN. The training process starts with data from the ground truth (labeled as 1 or positive, where deformation is present; and 0 or negative in other areas eg: background). Data augmentation has been done to balance the number of Positive and negative samples for training CNNs.

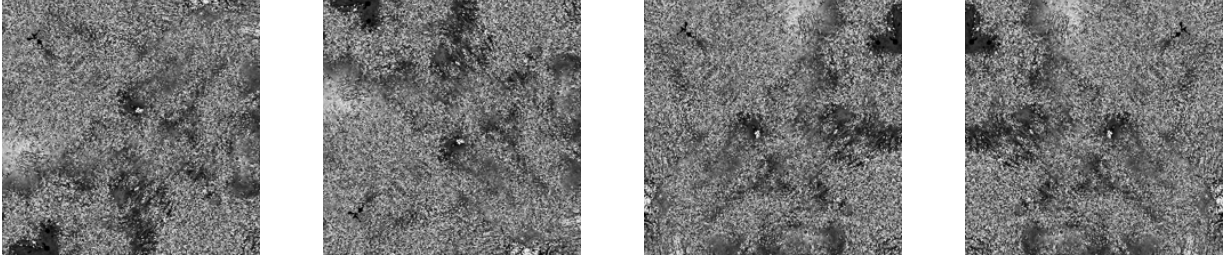


Figure 3: images from background class @source:Dataset

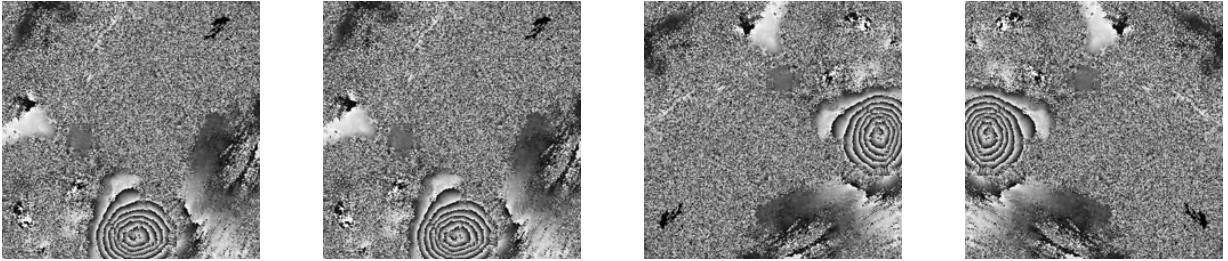


Figure 4: images from volcano deformation class @source:Dataset

4.1 Our data and Preparation

In our case data we are dealing with is from mining deformation(SSD). Unlike volcano data, our data has less Signal-to-noise ratio. Since the scale of Deformation is small, fringes are less significant and weak. Since The amount of data available is quite less compared to volcanic deformation, it is being augmented. Machine learning models are better when trained on a sufficient amount of training data, and CNN models are designed to work well in the case of small training data and have better accuracy with fewer training parameters.

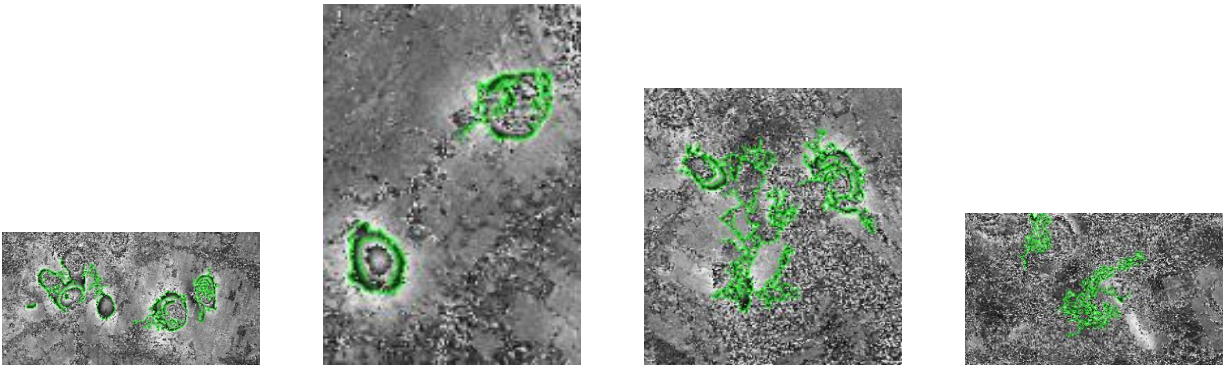


Figure 5: images from mining Deformation interferograms using canny edge detection, The leftmost image patch is Noise that is detected as a fringe, Also sizes are varying from image to image

4.2 Challenges involved

In the Mining data set, we have applied a Gaussian filter to remove noise and canny edges detection algorithms to detect edges. Two challenges involved in this process are

1. The amount of training data available is low
2. Fringes in low SNR region remain undetected for some threshold levels which varies from image to image
3. Some Noisy regions are detected as fringe.(eg: leftmost image)
4. Size and Dimension of croppings vary significantly, on the other hand, CNNs can take images of any size but the fully connected layers should have fixed size input,(to overcome this issue SPPnets are used)
5. Unlike Volcanic Deformation, Fringe patterns and shapes vary widely across the images and it is comparatively difficult For CNNs to learn those patterns.
6. These patterns sometimes are connected to each other and are Merged together unlike Volcanic Deformation fringes.

5 LITERATURE REVIEW

To learn about thousands of objects from millions of images, we need a model with a large learning capacity. However, the immense complexity of the object recognition task implies that this problem cannot be specified even by a dataset as large as ImageNet, so a model should also have lots of prior knowledge to compensate for all the data we don't have[9]

Convolutional Neural Networks (CNNs) constitute one such class of models. Their learning capability and capacity can be controlled by varying their depth and breadth, and they also make strong and more accurate assumptions about the nature of images (namely, stationarity of statistics and locality of pixel dependencies)[9]. Thus, compared to standard feed-forward Neural Networks(NN) with similarly-sized layers, CNNs have much fewer connections and parameters so they are easier to train, while their theoretically best performance is likely to be only slightly worse[7,9]. Pooling layers in CNNs summarize the outputs of neighboring groups of neurons in the same kernel map. To some extent, this helps the models overcome object localization problems [7,9].

5.1 Hyper-parameters

A common problem faced is choosing a learning rate and optimizer (the hyper-parameters). hyper-parameters are crucial to training success, yet can be hard to find. It should be noted that the results below are for one specific model and dataset. The ideal hyper-parameters for other models and datasets might differ. Gradient descent is one of the most popular algorithms to perform optimization and by far the most common way to optimize neural networks. The Optimizers available in Keras API include Stochastic gradient descent(SGD), Root Mean Square Propagation(RMSprop), Adaptive Gradient descent(Adagrad), Adadelata, Adam, Adamax, and Nadam optimizers. It has to be noted that the choice of optimizers and learning rate for that particular optimizer has a great effect on training time and average accuracy on validation data. In our case, we tested the Model's performances with Adadelata, and SGD Optimizers with learning initial Learning rates(LR) of 0.1,0.01,0.001,0.0002,0.0005,0.0001.

while the default LR of Adadelta is 1.0, we tested it for the case of 0.01,0.1. It was observed that SGD is taking comparatively less time to update each gradient in an epoch. So, SGD Optimizer was chosen later for training all models. SGD performs frequent updates with a high variance that causes the objective function to fluctuate heavily. So the Testing loss is often seen fluctuating, while the fluctuations in Validation accuracy can be due to overfitting sometimes. SGD’s fluctuation, on the one hand, enables it to jump to new and potentially better local minima[2]. On the other hand, this ultimately complicates convergence to the exact minimum, as SGD will keep overshooting.

lr=0.001, decay=1e-6, momentum=0.9, nesterov=True were given as input parameters for SGD in all cases and each model is trained for 20 epochs, (Alexnet for 50 epochs). A kernel Regularizer with L_2 , (0.01 as input parameter) is chosen on a Dense layer with 200 Neurons in a Fully Connected Layer(FCL)on top of the CNN block for each model. This helps in reducing Fluctuations in training Loss, accuracy, and chance of overfitting.

5.2 Activations

The standard way to model a neuron’s output f as a function of its input x is with $f(x) = \tanh(x)$ or $f(x) = (1 + e^x)^{-1}$ (sigmoid). In terms of training time with gradient descent, these saturating nonlinearities are much slower than the non-saturating nonlinearity $f(x) = \max(0, x)$ (ReLU)[9]. Deep convolutional neural networks with ReLUs train several times faster than their equivalents with *tanh* or *Sigmoid* units.ReLUs have the desirable property that they do not require input normalization to prevent them from saturating. If at least some training examples produce a positive input to a ReLU, learning will happen in that neuron. In our training, we often used a combination of these activations to test the model on the Volcanic deformation dataset. At fully connected layers on the top, we used *softmax* activation which pushes all the outputs in the range of $[0,1]$ as class probabilities.

5.3 DropOut

Combining the predictions of many different models is a very successful way to improve test accuracy, but it can be computationally too expensive for big neural networks (with More parameters and Deeper) to train. There is, however, a very efficient way of model combination that only costs about a factor of two during training, called “dropout”, which consists of setting the output of each hidden neuron to zero with a probability p given as a parameter to Dropout layer. The neurons that are “dropped out” in this way do not contribute to the forward pass and do not participate in backpropagation as well. So every time an input is given to the Network, the neural network effectively samples a different architecture[9], but all these architectures share weights. This technique reduces complex co-adaptations of neurons since a neuron cannot rely on the presence of particular other neurons. It is, therefore, forced to learn more robust features that are useful in conjunction with many different random subsets of the other neurons[9]. At test time, we use all the neurons but multiply their outputs by p , which is a reasonable approximation to taking the geometric mean of the predictive distributions produced by the exponentially many dropout networks. In our work, we chose Dropout as 0.5 in the 2nd last layer of FCLs and 0.2,0.3 in initial experimentation with some Models.

5.4 Transfer learning

Transfer learning is a machine learning method where a model developed for a task is reused as the starting point for a model on a second task. For image classification of problems, it is common to use a deep learning model pre-trained for a large and challenging image classification task such as the ImageNet 1000-class photograph classification competition. Many deep neural networks trained on natural images are known to exhibit a curious phenomenon in common: on the first layer, they learn features similar to Gabor filters and color blobs[3]. Such first-layer features appear not to be specific to a particular dataset or task, but general in that they are applicable to many datasets and tasks. In our problem, we used and tested the transfer learning strategy with different models whose weights are loaded from models trained on the Imagenet data set. Transfer learning worked well with VGG16, and InceptionV3 but failed in the case of ResNet and DenseNets for a Learning rate of 0.001 and 20epochs. The performance of these models is shown in the Results section.

5.5 SPPNet

The most important challenge with our Dataset is overcoming the issue of varying input sizes. Convolutional Blocks can take inputs of any dimension but the Top layers of these models i.e. The FCLs can only take input vectors of fixed size. To deal with this issue, we used the Spatial Pyramid pooling (SPP) layer on top of the CNN block. These work by fixing the number of bins per image with Varying bin sizes. Fixing Number bins per a feature map ensures the input shape to Dense layers of the network is invariant[4]. SPPlayer takes input from a list(eg:[2,4,6])as input argument and outputs a

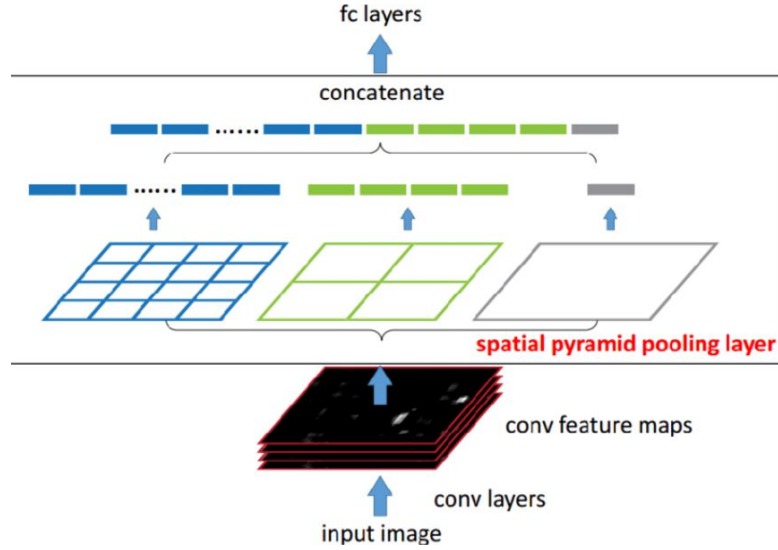


Figure 6: Figure showing SPP Layer working @source: [4]

one-dimensional vector of size sum of the squares of the input list(i.e $56=2^2 + 4^2 + 6^2$ in our example)

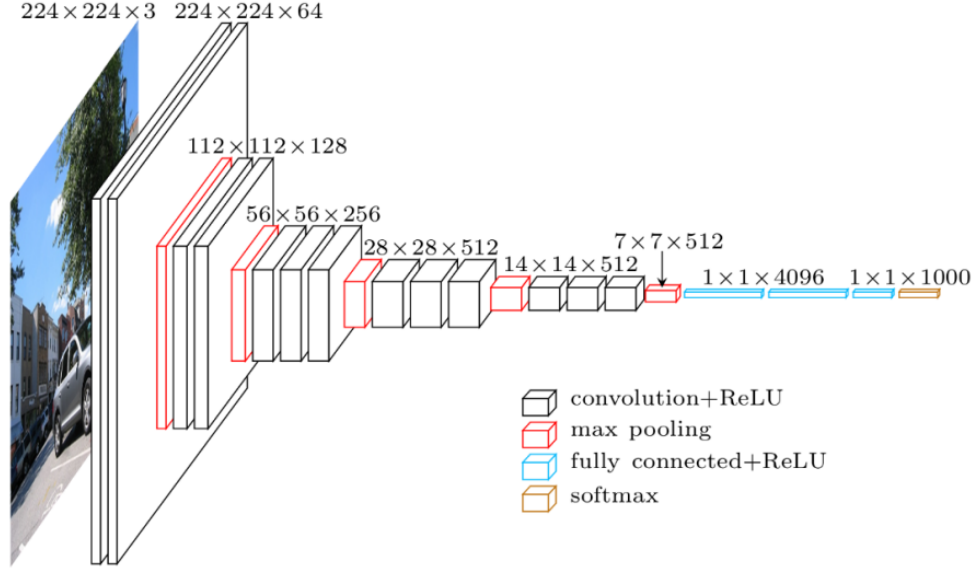


Figure 7: Figure showing VGG16 architecture @source :[1]

5.6 CNN Models used and their Architectures

VGG16 is a convolutional neural network model proposed by K. Simonyan and A. Zisserman from the University of Oxford in the paper “Very Deep Convolutional Networks for Large-Scale Image Recognition”. The model achieves 92.7(%) top-5 test accuracy in ImageNet, which is a dataset of over 14 million images belonging to 1000 classes.

Unfortunately, there are two major drawbacks with VGGNet:

1. It is painfully slow to train.
2. The network architecture weights themselves are quite large (concerning disk/bandwidth).

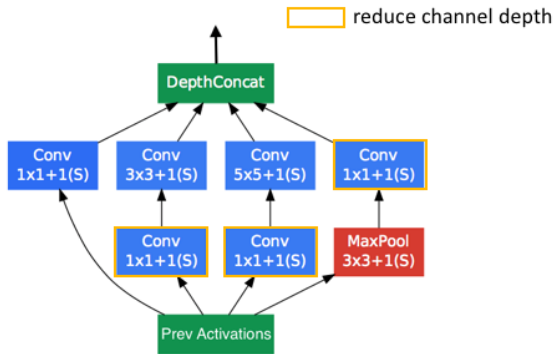


Figure 8: Inception Cell @source : [1]

In 2014, researchers at Google introduced the Inception network. The model is comprised of a basic unit referred to as an “Inception cell” in which we perform a series of convolutions at different scales and subsequently aggregate the results. For each cell, we learn a set of 1x1, 3x3, and 5x5 filters which can learn to extract features at different scales from the input. Max pooling is also used, albeit with “same” padding to preserve the dimensions so that the output can be properly concatenated.

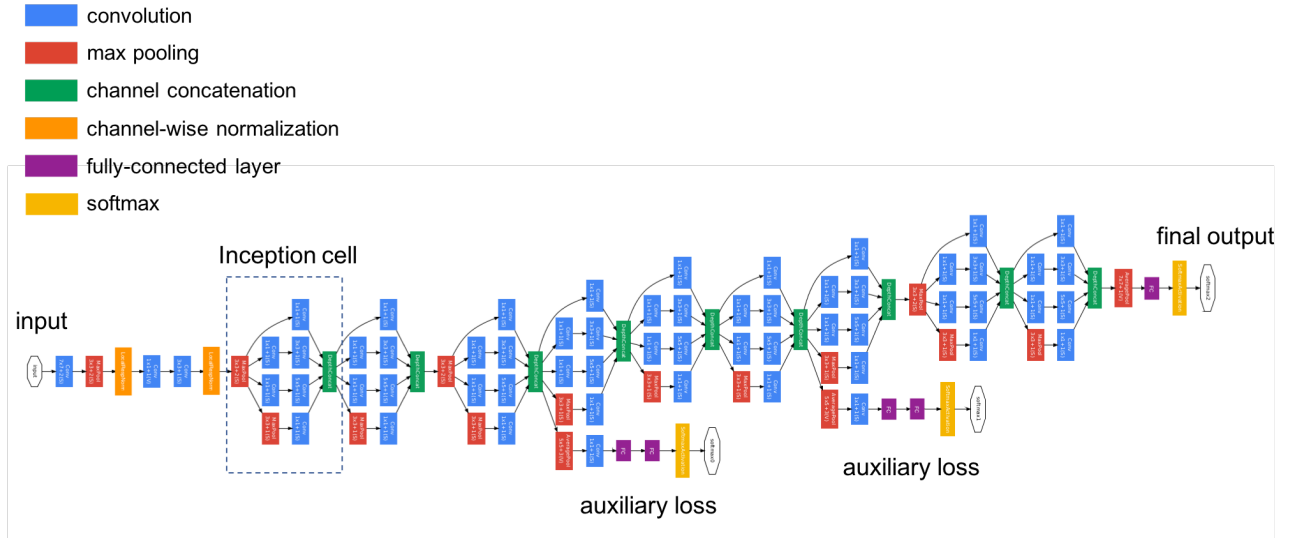
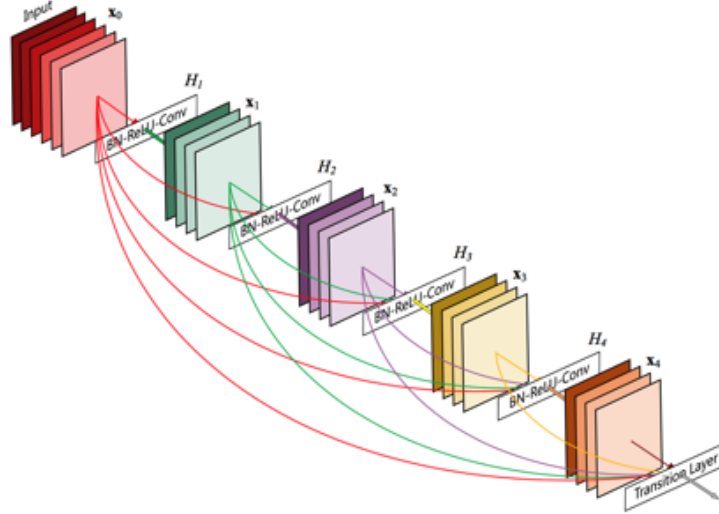


Figure 9: Figure showing CNN block of InceptionV3 @source: [1]

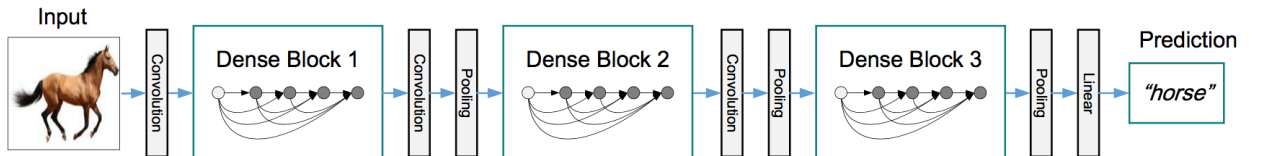


Figure 10: Figure showing CNN block of ResNet, ResNets are easy to optimize, but the “plain” networks (that simply stack layers) show higher training error when the depth increases. ResNets can easily gain accuracy from greatly increased depth, producing results that are better than previous networks. It is worth noticing that the ResNet model has fewer filters and lower complexity than VGG nets.



ht

Figure 11: Figure showing Dense block of DenseNet121, To further, improve the information flow between layers a different connectivity pattern has been proposed. Dense blocks are Designed to have direct connections from any layer to all subsequent layers. Traditional convolutional feed-forward networks connect the output of the L^{th} layer as input to the $(L + 1)^{th}$ layer, which gives rise to the following layer transition: $x_l = H_l(x_{l-1})$. ResNet add a skip-connection that bypasses the non-linear transformations with an identity function: $x_l = H_l(x_{l1}) + x_{l-1}$ [8]. In the case of DenseNets, it is $x_l = H_l([x_0, x_1, ..., x_{l-1}])$, where $[x_0, x_1, ..., x_{l-1}]$ is the concatenation of all previous layers [5].



ht

Figure 12: Figure showing CNN block of DenseNet121 @source : [1]

5.6.1 AlexNet

In AlexNet(A plain neural net), the Relu activation function is used instead of *Tanh* to add non-linearity. It accelerates the speed by 6 times at the same accuracy. Uses dropout instead of regularisation to deal with overfitting. However, the training time is doubled with the dropout rate of 0.5. overlap pooling to reduce the size of the network. It reduces the top-1 and top-5 error rates by 0.4% and 0.3%, respectively (on a dataset with enough classes). It has 5 Convolutional layers, 3 FCL, and a total of 62,378,344 parameters to train [4].

5.6.2 VGG16

Layer (type)	Output Shape	Param #
VGG16 (Model)	(None, 200)	15445000
dense_8 (Dense)	(None, 200)	40200
batch_normalization_4 (Batch Normalization)	(None, 200)	800
activation_4 (Activation)	(None, 200)	0
dense_9 (Dense)	(None, 200)	40200
batch_normalization_5 (Batch Normalization)	(None, 200)	800
activation_5 (Activation)	(None, 200)	0
dropout_2 (Dropout)	(None, 200)	0
dense_10 (Dense)	(None, 2)	402
batch_normalization_6 (Batch Normalization)	(None, 2)	8
activation_6 (Activation)	(None, 2)	0
Total params: 15,527,410		
Trainable params: 15,526,606		
Non-trainable params: 804		

Figure 13: Table showing VGG16's summary;On top of CNN block custom dense layers(FCLs) were added. @source:output log

Layer (type)	Output Shape	Param #
=====	=====	=====
model_2 (Model)	(None, 200)	15445000
dense_8 (Dense)	(None, 200)	40200
batch_normalization_4 (Batch Normalization)	(None, 200)	800
activation_4 (Activation)	(None, 200)	0
dense_9 (Dense)	(None, 200)	40200
batch_normalization_5 (Batch Normalization)	(None, 200)	800
activation_5 (Activation)	(None, 200)	0
dropout_2 (Dropout)	(None, 200)	0
dense_10 (Dense)	(None, 2)	402
batch_normalization_6 (Batch Normalization)	(None, 2)	8
activation_6 (Activation)	(None, 2)	0
=====	=====	=====
Total params: 15,527,410		
Trainable params: 12,610,958		
Non-trainable params: 2,916,452		

Figure 14: Table showing Pretrained VGG16's summary; On top of CNN block custom dense layers (FCIs) were added, and some CNN layers were Freezed from learning. @source:output log

5.6.3 InceptionV3

Layer (type)	Output Shape	Param #
=====	=====	=====
InceptionV3 (Model)	(None, 200)	24105960
dense_98 (Dense)	(None, 200)	40200
batch_normalization_246 (Batch Normalization)	(None, 200)	800
activation_1128 (Activation)	(None, 200)	0
dense_99 (Dense)	(None, 200)	40200
batch_normalization_247 (Batch Normalization)	(None, 200)	800
activation_1129 (Activation)	(None, 200)	0
dropout_20 (Dropout)	(None, 200)	0
dense_100 (Dense)	(None, 2)	402
batch_normalization_248 (Batch Normalization)	(None, 2)	8
activation_1130 (Activation)	(None, 2)	0
=====	=====	=====
Total params: 24,188,370		
Trainable params: 24,153,134		
Non-trainable params: 35,236		

Figure 15: Table showing InceptionV3 summary. On top of the CNN block custom dense layers (FCs) were added. @source:output log

Layer (type)	Output Shape	Param #
=====		
InceptionV3 (Model)	(None, 200)	24105960
dense_5 (Dense)	(None, 200)	40200
batch_normalization_189 (Batch Normalization)	(None, 200)	800
activation_189 (Activation)	(None, 200)	0
dense_6 (Dense)	(None, 200)	40200
batch_normalization_190 (Batch Normalization)	(None, 200)	800
activation_190 (Activation)	(None, 200)	0
dropout_1 (Dropout)	(None, 200)	0
dense_7 (Dense)	(None, 2)	402
batch_normalization_191 (Batch Normalization)	(None, 2)	8
activation_191 (Activation)	(None, 2)	0
=====		
Total params: 24,188,370		
Trainable params: 13,499,662		
Non-trainable params: 10,688,708		
=====		

Figure 16: Table showing Pretrained InceptionV3 summary. On top of the CNN block custom dense layers (FCs) were added. Some CNN layers were Frozen from learning. @source: output log

5.6.4 ResNet50

Layer (type)	Output Shape	Param #
Resnet50 (Model)	(None, 200)	25890888
dense_18 (Dense)	(None, 200)	40200
batch_normalization_195 (Batch Normalization)	(None, 200)	800
activation_729 (Activation)	(None, 200)	0
dense_19 (Dense)	(None, 200)	40200
batch_normalization_196 (Batch Normalization)	(None, 200)	800
activation_730 (Activation)	(None, 200)	0
dropout_3 (Dropout)	(None, 200)	0
dense_20 (Dense)	(None, 2)	402
batch_normalization_197 (Batch Normalization)	(None, 2)	8
activation_731 (Activation)	(None, 2)	0
Total params: 25,973,298		
Trainable params: 25,919,374		
Non-trainable params: 53,924		

Figure 17: Table showing ResNet50 summary, On top of CNN block custom dense layers (FCs) were added. @source: output log

Layer (type)	Output Shape	Param #
resnet50 (Model)	(None, 7, 7, 2048)	23587712
flatten_1 (Flatten)	(None, 100352)	0
dense_1 (Dense)	(None, 200)	20070600
batch_normalization_1 (Batch Normalization)	(None, 200)	800
activation_50 (Activation)	(None, 200)	0
dense_2 (Dense)	(None, 200)	40200
batch_normalization_2 (Batch Normalization)	(None, 200)	800
activation_51 (Activation)	(None, 200)	0
dropout_1 (Dropout)	(None, 200)	0
dense_3 (Dense)	(None, 2)	402
batch_normalization_3 (Batch Normalization)	(None, 2)	8
activation_52 (Activation)	(None, 2)	0
Total params: 43,700,522		
Trainable params: 23,527,558		
Non-trainable params: 20,172,964		

Figure 18: Table showing Pretrained ResNet50 summary, On top of CNN block custom dense layers(FCLs) were added. some CNN layers were Frozen from learning @source: output log

5.6.5 DenseNet121

Layer (type)	Output Shape	Param #
=====	=====	=====
DenseNet121 (Model)	(None, 200)	8292104
dense_3 (Dense)	(None, 200)	40200
batch_normalization_1 (Batch Normalization)	(None, 200)	800
activation_1 (Activation)	(None, 200)	0
dense_4 (Dense)	(None, 200)	40200
batch_normalization_2 (Batch Normalization)	(None, 200)	800
activation_2 (Activation)	(None, 200)	0
dropout_1 (Dropout)	(None, 200)	0
dense_5 (Dense)	(None, 2)	402
batch_normalization_3 (Batch Normalization)	(None, 2)	8
activation_3 (Activation)	(None, 2)	0
=====	=====	=====
Total params: 8,374,514		
Trainable params: 8,290,062		
Non-trainable params: 84,452		

Figure 19: Table showing DenseNet121 summary, On top of CNN block custom dense layers (FCs) were added. source: output log

Layer (type)	Output Shape	Param #
DenseNet121 (Model)	(None, 200)	8292104
dense_3 (Dense)	(None, 200)	40200
batch_normalization_1 (Batch Normalization)	(None, 200)	800
activation_1 (Activation)	(None, 200)	0
dense_4 (Dense)	(None, 200)	40200
batch_normalization_2 (Batch Normalization)	(None, 200)	800
activation_2 (Activation)	(None, 200)	0
dropout_1 (Dropout)	(None, 200)	0
dense_5 (Dense)	(None, 2)	402
batch_normalization_3 (Batch Normalization)	(None, 2)	8
activation_3 (Activation)	(None, 2)	0
Total params: 8,374,514		
Trainable params: 7,278,606		
Non-trainable params: 1,095,908		

Figure 20: Table showing Pretrained DenseNet121 summary, On top of CNN block custom dense layers(Fcls) were added.some CNN layers were Frozen from learning @source: output log

6 HARDWARE ACCELERATORS and LIBRARIES

Keras API is extensively used for building All CNN models. All the models were trained on Google Colab. Colab provides a virtual machine for each session that can last up to 12hrs, and 90 mins of idle time. For every 12hrs Disk, RAM, VRAM, CPU cache, etc data that is on our allotted virtual machine will get erased

GPU: 1xTesla T4, 2560 CUDA cores, 320 Tensor Cores, compute 3.7, 16GB of (14.56 usable)GDDR6 VRAM,8.1 TFLOPS single-precision floating-point performance

CPU: 1xsingle core hyperthreaded i.e(1 core, 2 threads) Xeon Processors @2.3Ghz (No Turbo Boost), 45MB Cache

RAM: 12.6 GB Available

Disk: 320 GB Available

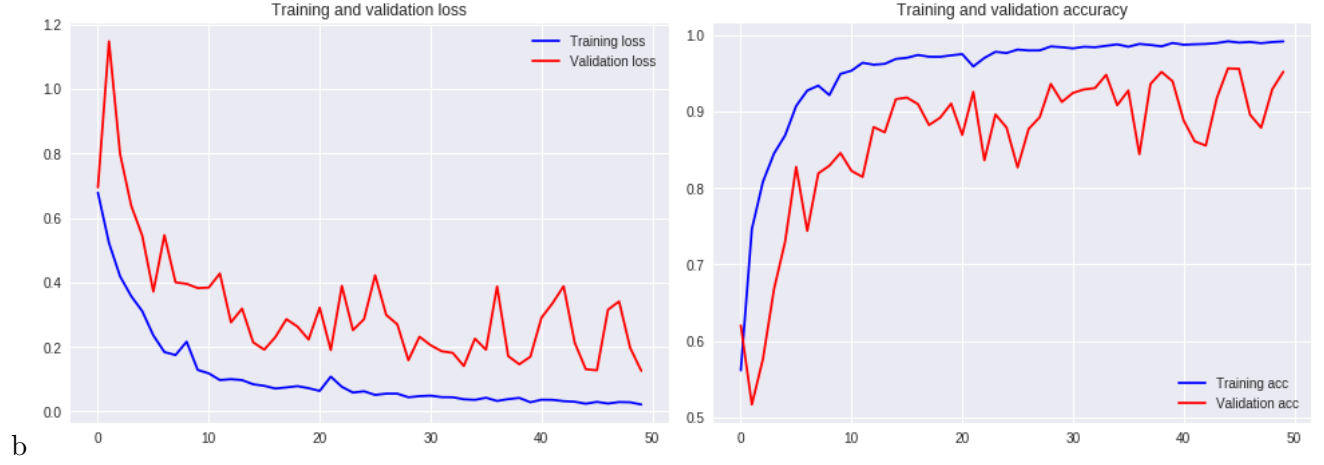


Figure 21: Alexnet performance, LR=0.01,SGD ,50 epochs;8:2 validation split(22745+5685 images)

7 RESULTS

The following plots were obtained by plotting the history of trained models. Sparse categorical cross entropy was chosen as the loss function, (binary classification problem, binary cross entropy is same as this for our case). All the models were trained for 20 epochs, on Google Colab. The dataset contains 28430 images of 2 classes(Background and Volcanic deformation) roughly equal number of images in each class. Transfer learning the strategy was used with pre-trained models. pre-trained weights are from model weights of Imagenet Data. Transfer learning strategy works perfectly well with, VGG16, and InceptionV3 but not in the case of ResNet50 and DenseNet121.

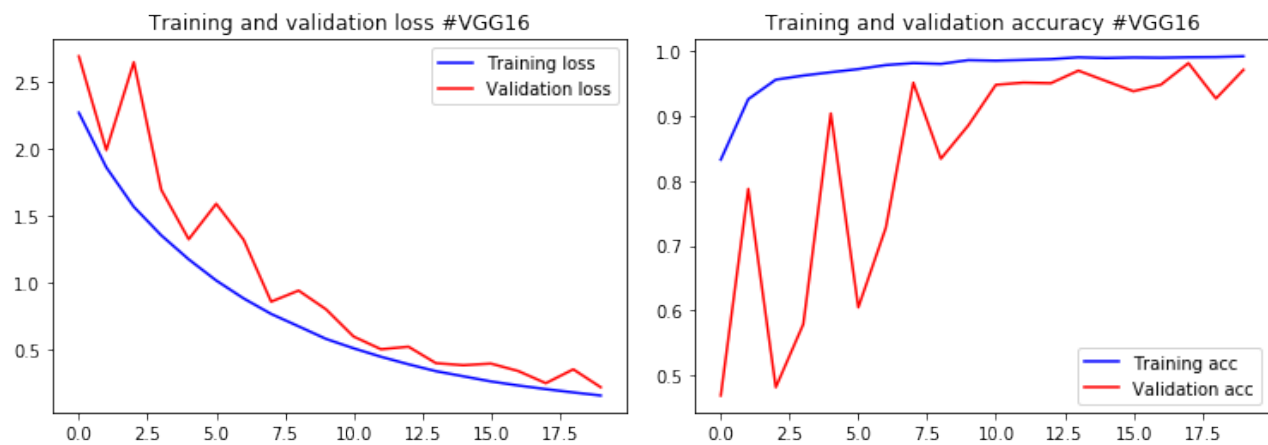


Figure 22: VGG16 performance, LR=0.001,SGD ,20 epochs;8:2 validation split(22745+5685 images)

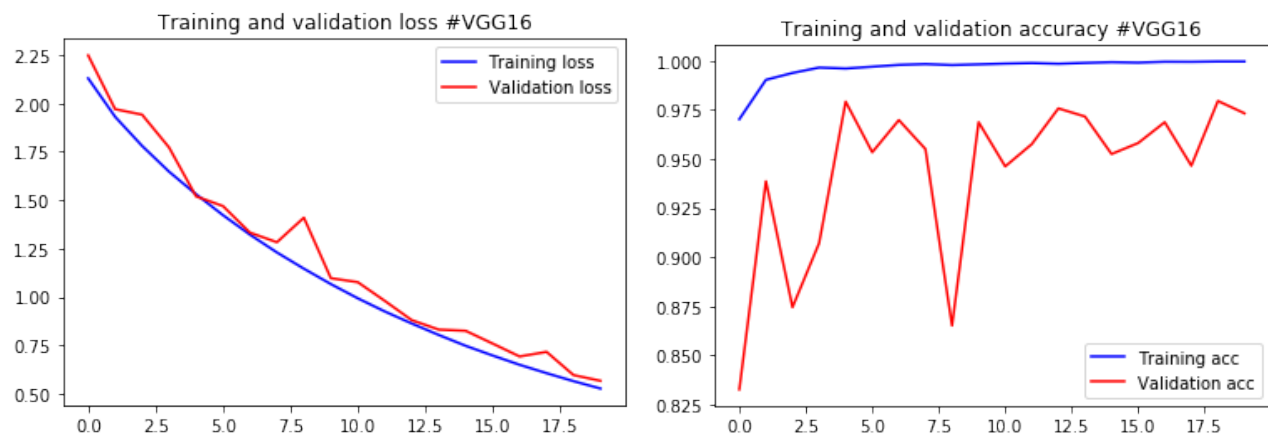


Figure 23: Pretrained VGG16 performance, LR=0.001,SGD ,20 epochs;8:2 validation split(22745+5685 images)

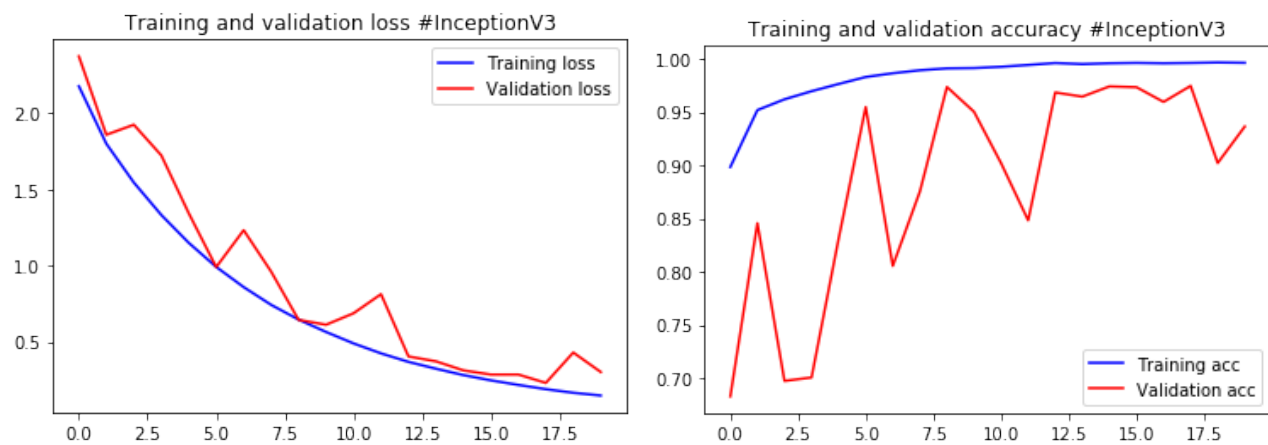


Figure 24: InceptionV3 Performance, LR=0.001,SGD ,20 epochs;8:2 validation split(22745+5685 images)

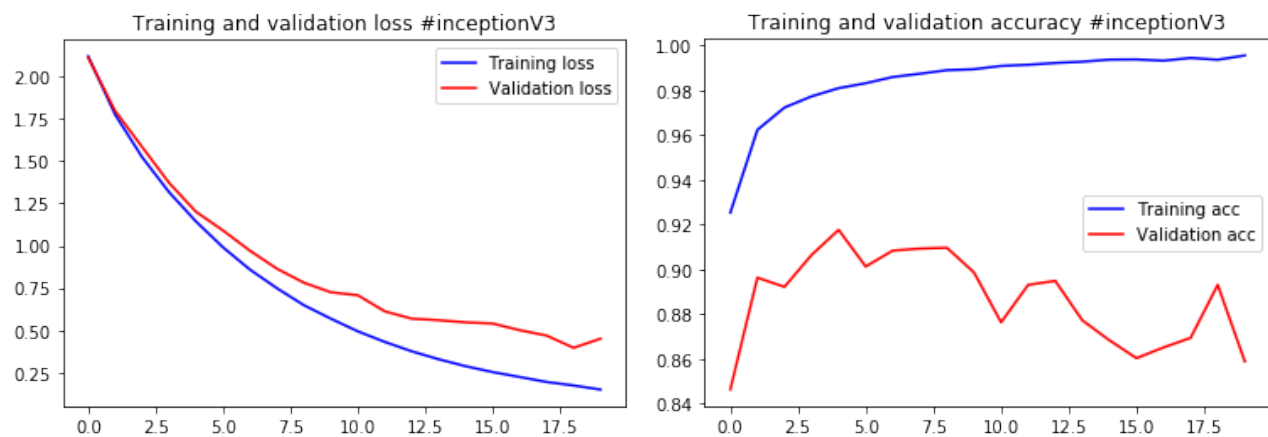


Figure 25: Pretrained InceptionV3 Performance, LR=0.001,SGD ,20 epochs;8:2 validation split(22745+5685 images), pre-trained on Imagenet dataset

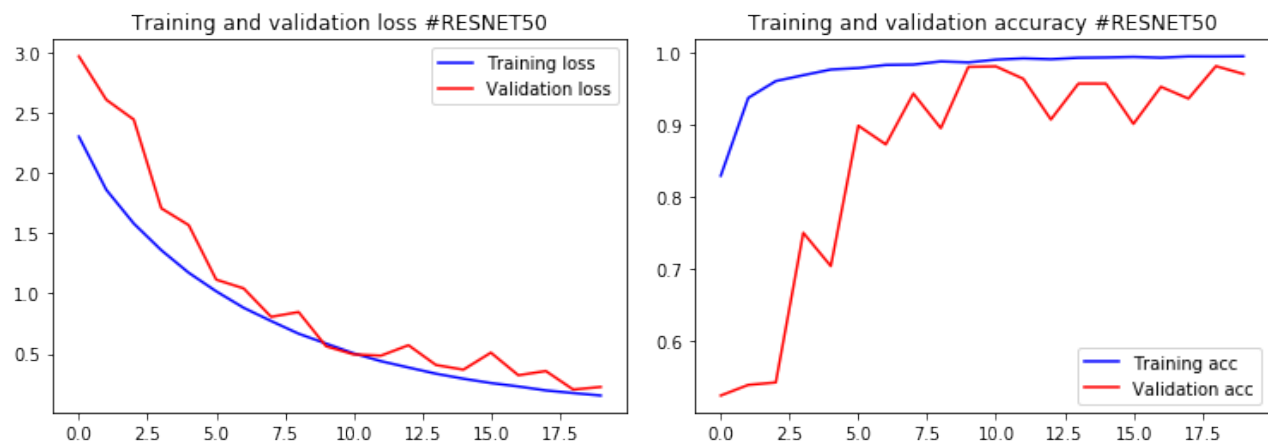


Figure 26: ResNet50 Performance, LR=0.001,SGD ,20 epochs;8:2 validation split(22745+5685 images)

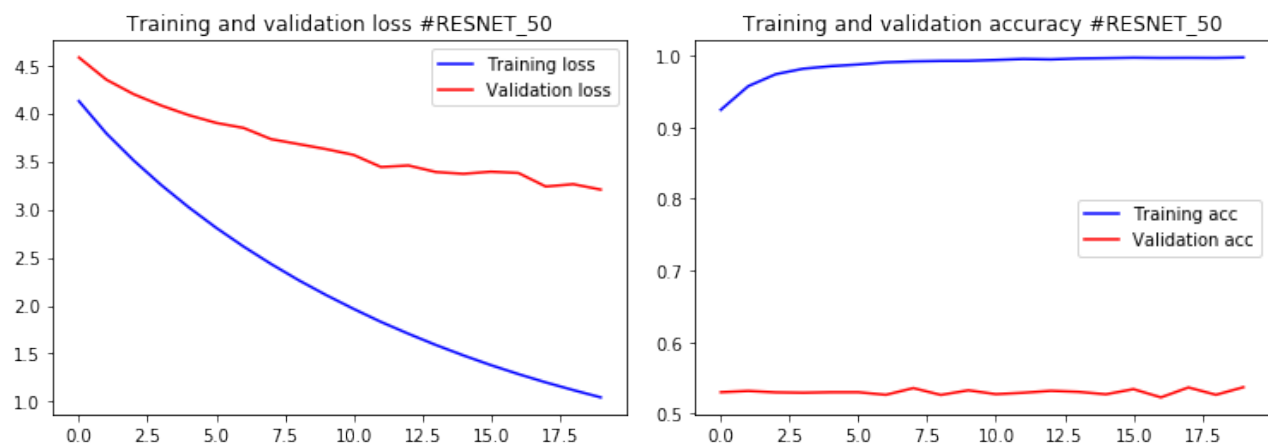


Figure 27: ResNet50 Performance, LR=0.001,SGD ,20 epochs;8:2 validation split(22745+5685 images),pre-trained on Imagenet dataset

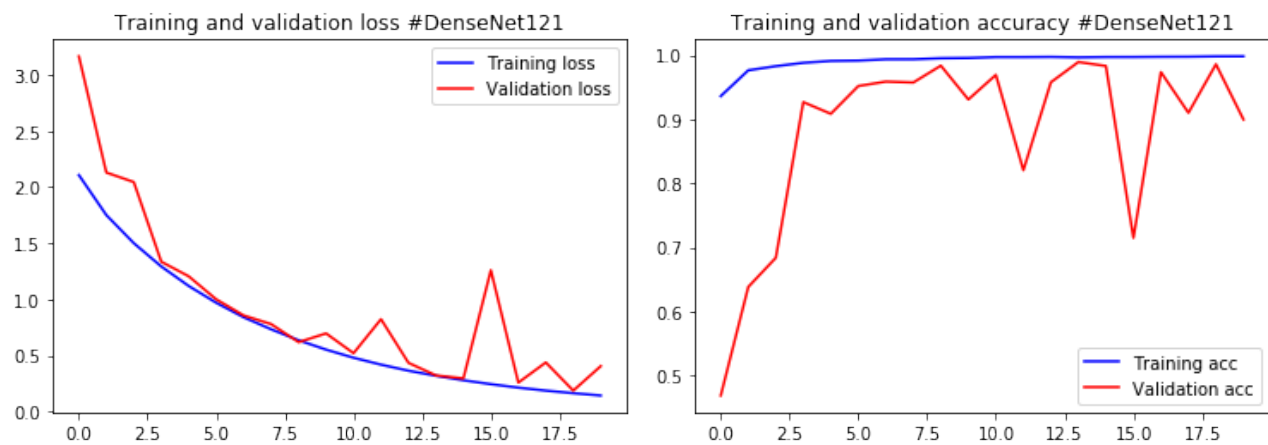


Figure 28: DenseNet Performance, LR=0.001,SGD ,20 epochs;8:2 validation split(22745+5685 images)

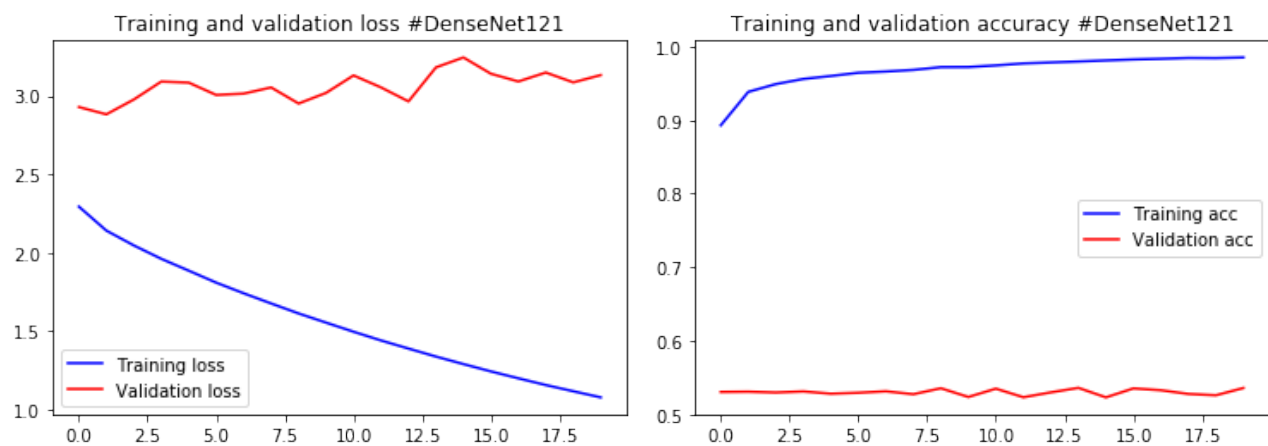


Figure 29: Pretrained DenseNet121 Performance, LR=0.001,SGD ,20 epochs;8:2 validation split(22745+5685 images),pre-trained on Imagenet dataset

Summary of Results, trained on volcano dataset, 28430 images ($224 \times 224 \times 3$)							
CNN	Epochs	Learning Rate	Time per epoch	validation split	Trainable parameters	Non trainable parameters	validation accuracy (%) avg
AlexNet	50	0.01	$\sim 220s$	0.2	62,378,344	—	93
VGG16	20	0.001	390s	0.2	15,526,606	804	95
VGG16-pretrained	20	0.001	312s	0.2	12,610,958	2,916,452	97
InceptionV3	20	0.001	354s	0.2	24,153,134	35,236	93
InceptionV3-Pretrained	20	0.001	300s	0.2	13,499,662	10,688,708	85
ResNet50	20	0.001	384s	0.2	25,919,374	53,924	97
ResNet50-pretrained	20	0.001	284s	0.2	23,527,558	20,172,964	53
Densenet121	20	0.001	390s	0.2	8,290,062	84,452	94
DenseNet121-pretrained	20	0.0005	335s	0.2	7,278,606	1,095,908	53

8 Inference and Continuation of work..

Now we have seen the performance of various CNN models on volcanic datasets, both in case of Pre-trained and learning from scratch. The following statements can be inferred from training the models

1. Transfer learning works most often but not always, particularly in the case of ResNet and DenseNets (both of which have connections from their previous layers in their fundamental blocks). It is believed that the Transfer learning strategy works well with data sets from similar domains but in our case imagenet dataset and Volcanic data are completely different domains still VGG16 and Inception worked pretty well. This could be due to the fact that CNN layers at the bottom learn the most generalized feature of a natural image.
2. Choice Hyperparameters greatly affect the model's overall performance.
3. The size of the network or the Number of parameters always does not always guarantee better performance. (DenseNets performed better than Resnets)
4. Higher batch size helps the model to better generalize. Note that an ideal model's performance should not depend on the order of inputs that we give. lower the batch size per epoch more possible ways of giving inputs, and less generalized is the model.

These trained models were saved in the model name.h5 file, and will be used for transfer learning in the Mining Dataset. The mining dataset should be trained with SPPlayer on top of the CNN block. Multisized training should be done to make the model learn better.

9 References

- [1]Jeremy Jordan,19 APRIL 2018, Article title: "Common architectures in convolutional neural networks."
- [2]Sebastian Ruder,19 JANUARY 2016, Article title: "An overview of gradient descent optimization algorithms"
- [3]Jason Yosinski,1 Jeff Clune,2 Yoshua Bengio,3 and Hod Lipson4, "How transferable are features in deep neural networks?"arxiv:1411.1792
- [4]Kaiming He, Xiangyu Zhang, Shaoqing Ren, and Jian Sun "Spatial Pyramid Pooling in Deep Convolutional Networks for Visual Recognition"arXiv:1406.4729
- [5] Gao Huang Cornell University,Zhuang Liu Tsinghua University,Laurens van der Maaten,Kilian Q. Weinberger "Densely Connected Convolutional Networks"arXiv:1608.06993
- [6]Christian Szegedy, Vincent Vanhoucke, Sergey Ioffe, Jonathon Shlens, Zbigniew Wojna "Rethinking the Inception Architecture for Computer Vision"arXiv:1512.00567
- [7]Karen Simonyan, Andrew Zisserman,"Very Deep Convolutional Networks for Large-Scale Image Recognition"arXiv:1409.1556
- [8]Kaiming He, Xiangyu Zhang, Shaoqing Ren, Jian Sun"Deep Residual Learning for Image Recognition" arXiv:1512.03385
- [9]Alex Krizhevsky, Ilya Sutskever, Geoffrey E. Hinton"ImageNet Classification with Deep Convolutional Neural Networks"[2012]
- [10]N. Anantrasirichail , J. Biggs2 , F. Albino2 , P. Hill1, and D. Bull1 "Application of Machine Learning to Classification of Volcanic Deformation in Routinely Generated InSAR Data"AGU100 Research article:10.1029/2018JB015911
- [11] Ullaby book, Chapter 14, Real Synthetic Aperture radar side looking airborne Radar